Research article

Journal of MASS SPECTROMETRY

Received: 25 September 2012 Revised: 27 March 2013 Accepted: 27 March 2013 Published online in Wiley Online Library

(wileyonlinelibrary.com) DOI 10.1002/jms.3212

Direct desorption/ionization of analytes by microwave plasma torch for ambient mass spectrometric analysis

Tiqiang Zhang,[a,b] Wei Zhou,[c] Wei Jin,[a] Jianguang Zhou,[a] Eric Handberg,[c] Zhiqiang Zhu,[c]* Huanwen Chen[c] and Qinhan Jin[a,b]*

Ambient ionization is the new revolution in mass spectrometry (MS). A microwave plasma produced by a microwave plasma torch (MPT) at atmospheric pressure was directly used for ambient mass spectrometric analysis. H_3O^+ and NH_4^+ and their water clusters from the background are formed and create protonated molecules and ammoniated molecules of the analytes. In the full-scan mass spectra, both the quasi-molecular ions of the analytes and their characteristic ionic fragments are obtained and provide evidence of the analyte. The successful detection of active compounds in both medicine and garlic proves that MPT has the efficient desorption/ionization capability to analyze solid samples. The obtained decay curve of nicotine in exhaled breath indicates that MPT-MS is a useful tool for monitoring gas samples in real time. These results showed that the MPT, with the advantages of stable plasma, minimal optimization, easy, solvent-free operation, and no pretreatment, is another potential technique for ambient MS. Copyright © 2013 John Wiley & Sons, Ltd.

Supporting information may be found in the online version of this article.

Keywords: microwave plasma torch; desorption; ionization; ambient; mass spectrometry

Introduction

Mass spectrometry (MS) is one of the most successful analytical techniques, providing high sensitivity, selectivity, and speed[1] for chemical analysis. A contemporary revolution was the development of ambient ionization techniques, which enabled the ionization of samples in their native environment without sample pretreatment and increased throughput.[2] After the emergence of the pioneered technique, desorption electrospray ionization,[3] more than 20 direct-ionization techniques have been developed.[1,4–7] Among these techniques, several ionization methods including direct analysis in real time (DART),[8] desorption atmospheric pressure chemical ionization,[9] dielectric barrier discharge ionization,[10] plasma-assisted desorption ionization (PADI),[11] flowing atmospheric pressure afterglow (FAPA),[12] low-temperature plasma ionization,[13] atmospheric pressure ultrahigh frequency (UHF) plasma jet ionization,[14] microplasma discharge ionization,[15] and desorption corona beam ionization[16] were based on the atmospheric plasmas. A recent review[6] compares the plasma sources. In DART, desorption atmospheric pressure chemical ionization, and dielectric barrier discharge ionization, they use DC voltage (usually several kilovolts) to produce nearly invisible plasmas; therefore, positing sampling accurately on the surface is difficult. Obviously, sample placement improves with the visible plasma, and the visible plasma is achieved and is available in PADI, low-temperature plasma, atmospheric pressure UHF plasma jet ionization source, FAPA, microplasma discharge ionization source, and desorption corona beam ionization. Among them, the latter three use high AC voltage (hundreds of volts–several kilovolts) to generate plasma. To the best of our knowledge, the highest frequency currently used is 850 MHz in atmospheric pressure UHF plasma jet,[14] and the much more higher frequency has not been employed in an ambient ionization technique, because high-frequency components are unavailable.

As a new high-frequency plasma source, the microwave plasma torch (MPT), although not mentioned in the review, was developed initially at Jilin University[17] and was substantially promoted at Indiana University.[18] MPT easily generates a stable and visible flame-like plasma at atmospheric pressure and operates at 2450 MHz, a commercial microwave frequency, by which the plasma operation was significantly improved.[19] MPT offered a much better analytical performance for the introduction of aqueous aerosols. In the 1990s, various sample introduction methods as well as spectroscopic techniques based on the MPT were successfully introduced.[20,21] In addition, the MPT can be sustained in a variety of supporting gases, including Ar, He, N_2, Ne, and air.[22,23] The MPT is similar to inductively coupled plasma (ICP),

* *Correspondence to: Zhiqiang Zhu, Jiangxi Key Laboratory for Mass Spectrometry and Instrumentation, East China Institute of Technology. E-mail: zhiqiangzhu628496@gmail.com*

* *Correspondence to: Qinhan Jin, Research Center for Analytical Instrumentation, Zhejiang University. Email: qhjin@zju.edu.cn*

a *Research Center for Analytical Instrumentation, Institute of Cyber Systems and Control, State Key Laboratory of Industrial System and Control, Zhejiang University, Hangzhou 310027, China*

b *Department of Chemistry, Zhejiang University, Hangzhou 310027, China*

c *Jiangxi Key Laboratory for Mass Spectrometry and Instrumentation, East China Institute of Technology, Nanchang 330013, China*

but the plasma is smaller, and the MPT was mainly used as an excitation source for atomic emission spectrometry, portable spectrometer,[24,25] supercritical fluid chromatography,[20] and liquid chromatography,[26] for elemental analysis until the MPT temperature reported from some labs[19,27] was placed below the ICP temperature. The plasma temperature defines the atomization efficiency for atomic spectroscopy, so the ICP-MS is preferred over the MPT for atomic spectroscopy. Also, the plasma temperature defines the ionization efficiency. Although the ionization efficiency of ICP approaches 100% for atoms, the ionization efficiency of MPT is less than 100%. Still, molecular analysis should not break the chemical bonds of a molecule, so MPT researchers used MPT as an ionization source in MS[22,28–30] mainly for the element analysis. In addition, a helium MPT was coupled to time-of-flight mass spectrometer (TOF-MS) for the detection of halogenated hydrocarbons separated by a capillary gas chromatography.[31] More application can refer to the outstanding book of Jankowski *et al.*[19] For these applications of MPT with MS, the samples were all introduced into the plasma through the central tube of the MPT by a carrier gas. However, the direct desorption/ionization of analytes by MPT at ambient conditions has not been reported to date. Moreover, in comparison with previous AC driving plasma methods using in ambient ionization as mentioned in the previous paragraph, MPT uses a much higher frequency with a higher plasma temperature. The higher frequency may benefit the formation of a more stable plasma, and the higher plasma temperature may promote to the desorption process of analytes.

Besides, the ionization mechanism for molecules in an MPT is unclear. Without an understanding of the ionization mechanism, application works for molecular analysis with an MPT still in a trial-and-error process. In this study, the direct desorption/ionization capability of the argon-sustained MPT was demonstrated and two primary ions, H_3O^+ and NH_4^+, and their water clusters were identified from the background of the MPT. The effect of the drying nitrogen from the mass spectrometer on the production of the protonated ions and the ammonium adduct ions of the analytes was discussed. The active components in an over-the-counter (OTC) medicine and plant product were detected, and the limits of detection (LODs) were determined. Also, the dynamic change of nicotine in the exhaled breath after smoking was monitored. The background analysis provides information about the ionization mechanism. These results show that argon-sustained MPT is a useful alternative ionization source for directly ambient sample analysis in MS.

Experimental section

Materials and chemicals

The 2450 MHz microwave generator (YY1-50 W-2450) and the coaxial line (SFCJ-50-9) were purchased from Nanjing Electronic Technology Co., Ltd., Nanjing, China. High purity argon (99.999%) and liquid nitrogen were purchased from Jingong Special Gas Ltd., Hangzhou, China. Acetone (AR) and acetic acid (AR) were purchased from Zhongtian Chemical Co., Ltd., Wuhan, China. The cigarettes and garlic were purchased from the local supermarket. The OTC medicine including iburprofen (100 mg) tablets, chlorphenamine maleate (4 mg) tablets, difenidol hydrochloride (25 mg) tablets, domperidone (10 mg) tablets, and compound mixture with acetaminophen (250 mg), caffeine (30 mg), pseudoephedrine hydrochloride (15 mg), and chlorpheniramine maleate (3 mg) capsules were purchased from the local pharmacy (more information about these medicines is shown in the Table S1 in the supporting information).

Configurations and operations of MPT

The home-built MPT was described previously but is reviewed briefly.[18,21] Figure 1 is a schematic drawing of the MPT, the sample, surface, capillary cover, and counter-current, annular flow of nitrogen around the capillary. The MPT consists of three tubes, the microwave input tube, argon flow in central tube, and argon flow in the intermediate tube. The outer tube is made of brass with an outer diameter of 26 mm and inner diameter of 22 mm. The intermediate tube (5.5 mm o.d and 4.5 mm i.d.) and central tube (3 mm o.d. and 2 mm i.d.) are made of copper. The Ar-working gas is introduced separately into both the intermediate and the central tubes; this design has been used previously.[27] The dual-flow system is beneficial to modify the plasma jet shape. Microwave voltage is connected from the power supply to the intermediate tube with a coaxial cable and solder. The microwaves propagate in the cavity between the intermediate and outer tubes. The plasma is started with a spark, which is created manually by a short circuit between the intermediate and the inner tubes. The visible plasma forms near the top opening of the MPT and extends into the air at atmospheric pressure. The microwave power used was 10 W. The argon flows in the intermediate and the central tubes were about 300 and 1000 ml/min, respectively. By using these three parameters, a stable, cone-shaped plasma jet was generated.

Mass spectrometry

The MPT was coupled to an atmospheric pressure ionization TOF-MS (Corsair, Analytica of Branford, Inc.), replacing the commercial one. The source voltages on the cylinder electrode, the endplate, and the capillary entrance were 0, −50, and −200 V, respectively. Although the ion source cover was removed, these voltages both maintained ion signal and were safe to the operators. For the vacuum optics, the skimmer and the offset voltage were set to −15 and −10 V. The radiofrequency voltage for both the sample and the background were 80 and 30 V. The voltage for the ion detector, positive ion mode, pulse A data acquisition function, and 1-spectrum per second spectra acquisition rate were adjusted through the Aviator software. Likewise, the software controlled both the temperature and the flow of drying nitrogen. The flow rates of the drying nitrogen were set to 0–3 l/min for acetone and acetic acid and 1.5 l/min for pharmaceuticals, garlic, and exhaled breath. And, the temperature of drying nitrogen was 125 °C for pharmaceuticals and 25 °C for other samples.

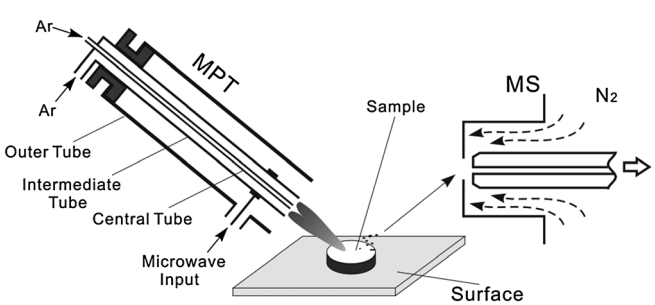

Figure 1. Schematic of the MPT ion source coupled to a TOF-MS.

Journal of MASS SPECTROMETRY

Sample analysis

Each OTC tablet or garlic was placed on a piece of glass plate and was exposed directly to the plasma. The MPT was positioned about 30 mm from the mass spectrometer ion inlet with an oblique angle of about 40° to the glass plate. The horizontal and vertical distances between the sample and the ion inlet of the mass spectrometer were 8 and 5 mm, respectively. When analyzing the exhaled breath, acetone vapor, and acetic acid vapor samples, the MPT was positioned horizontally and in-line with the inlet capillary, and the distance between the MPT and the ion inlet of mass spectrometer was about 30 mm. The gaseous samples were introduced at the midpoint.

Results and discussion

Background analysis of MPT

The overpopulation of high-energy electrons in the plasma generated by MPT makes the source attractive for analyte excitation and ionization.[27] A typical background spectrum obtained from MPT with argon and without drying nitrogen from the mass spectrometer is shown in Fig. 2. This background spectrum is some different from that of other plasma-based ionization sources, such as He-induced DART,[32] FAPA,[12] and microplasma,[15] and is also different from a radiation-based ionization source: beta electron-assisted direct chemical ionization probe.[33] In their spectra, the main peaks are usually at *m/z* 37 and 55, whereas the peaks at *m/z* 36 and 54 always have quite low abundance or even absent in He-induced DART.[32] The *m/z* 37 is usually the base peak for those ionization methods. In addition, the relative abundance of *m/z* 18 in these ambient ionization sources is very small or absent in microplasma[15] and BADCI.[33]

It is no doubt that *m/z* 19, 37, and 55 are the protonated water clusters ($(H_2O)_nH^+$, $n = 1–3$). In the Ar-MPT plasma region, the species such as Ar^*, $Ar^{\cdot+}$, and high-energy electrons are abundant. The internal energy of Ar^* and the ionization energy (IE) of $Ar^{\cdot+}$ are 11.7 and 15.8 eV, respectively. Thus, H_2O (IE = 12.6 eV) can be ionized by $Ar^{\cdot+}$ (not by Ar^*[34]) to be $H_2O^{\cdot+}$, which is sequent to form H_3O^+. Also, the high-energy electron is important to form $H_2O^{\cdot+}$ by direct collision or indirectly with $N_2^{\cdot+}$.[35] Although the ions of *m/z* 19, 37, and 55 are important proton supplier in ambient ionization source, but in Fig. 2, these ions have relatively low abundance, and the most abundant three ions are of *m/z* 18, 36, and 54. Thus, the ions of *m/z* 18, 36, and 54 are another series of important reactant ions in the MPT background. Here, they are suggested to be ammonium (*m/z* 18) and ammonium–water adducts (*m/z* 36 and 54). The ammonium may originate from two sources: (1) the trace amounts of ammonia in the laboratory environment and (2) formation by MPT. A simple experiment was performed. When pure N_2 or NH_3 was introducing into the interaction region of plasma, a new signal of *m/z* 35 was observed and was assigned to $NH_4^+ \cdot NH_3$. The ion–molecule complex increases significantly (e.g., about 10^5 cps) to the absolute intensity of the total ion current in Fig. 3. In principle, this observation supports this viewpoint. As far as well we know, this is the first observation of NH_4^+ ions in MPT. Although ammonia's formation mechanism is not clear yet, two other cases provide some evidences of the potential formation of ammonia. First, ammonia can be generated from N_2/H_2 through the microwave plasma.[36] Second, $[M + NH_4]^+$ is the main analyte ion in N_2-induced DART.[37] These two cases indicate that the ammonia is generated when N_2 is exposed to a discharge under certain conditions; thus, the formation of ammonia and ammonium by MPT is possible, and it was supported by the results shown in Fig. 3(a). The ions of *m/z* 18 and the water radical cation ($H_2O^{\cdot+}$) have the same mass, but $H_2O^{\cdot+}$ might convert quickly to H_3O^+ when water is present. Therefore, the ions of *m/z* 18 are more likely to be NH_4^+ rather than $H_2O^{\cdot+}$. In addition, NH_4^+ not only can be another proton source for the analytes with the higher proton affinity (PA) than NH_3 but also can form the adduct ion $[M + NH_4]^+$ with the PA lower but closer to NH_3.

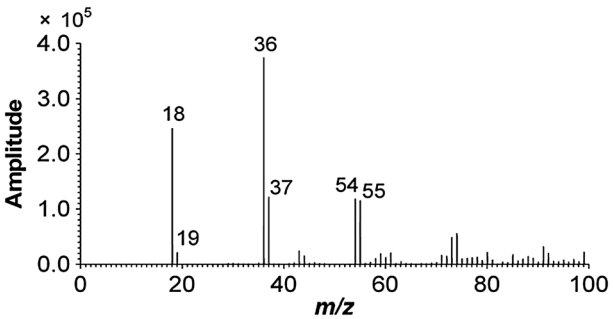

Figure 2. A typical mass spectrum of the background generated by MPT.

The conditions for generation of the two typical analyte ions $[M + H]^+$ and $[M + NH_4]^+$

The drying nitrogen from the mass spectrometer was found to be an important factor to affect the generation of the two typical analytet ions, the protonated molecules $[M + H]^+$ and the ammonium adducts $[M + NH_4]^+$. As shown in Fig. 4(a) and (c), for acetone, the single analyte ions $[M + NH_4]^+$ (*m/z* 76) and $[M + H]^+$ (*m/z* 59) were generated by adding 0 and 1.5 l/min drying nitrogen, respectively, but these two ions appeared simultaneously when 0.5 l/min drying nitrogen was used (Fig. 4(b)). This trend shows that at a low flow rate of drying nitrogen (0.5 l/min) or at no drying nitrogen, the ammonium adducts $[M + NH_4]^+$ are easily generated and are the main analyte ions. This acetone trend may be attributed to the amounts and characteristics of primary ions and the analytes. The PA of water, acetone, and ammonia are 691, 812, and 853.6 kJ/mol,[38] respectively. Among them, acetone's PA is far greater than water's; then, the proton transfers from the hydrated proton (or their water clusters) to acetone and forms the protonated acetone. When comparing with ammonia, acetone has a lower PA. Thus, proton transfer from NH_4^+ (or their ammonium–water clusters) to acetone cannot occur, but the ammonium adduct $[M + NH_4]^+$ will be formed for 787 kJ/mol < PA (acetone) < PA (ammonia).[39] Without drying nitrogen, the main primary ions from the background are $NH_4^+(H_2O)_n$ ($n = 0–2$) (Fig. 2), so they have a higher probability to encounter and react with acetone than $(H_2O)_nH^+$ ($n = 1–3$). Therefore, $[M + NH_4]^+$ is the predominant analyte ion without drying nitrogen (Fig. 4(a)).

While at a high flow rate of drying nitrogen, $[M + NH_4]^+$ ion disappeared, and the $[M + H]^+$ ions become the only analyte ions of acetone (Fig. 4(c)). These changes may be caused by two reasons. First, in the MPT background, the desolvation of the drying nitrogen promoted $H_3O^+(H_2O)_n$ ($n \geq 1$) to convert to H_3O^+ (Figure S1 in the Supporting Information), which then reacted with acetone and produced more protonated acetone ions $[M + H]^+$. Second, the binding of ions $[M + NH_4]^+$ for ketone is weak, and $[M + NH_4]^+$ was verified to dissociate to NH_4^+ as the

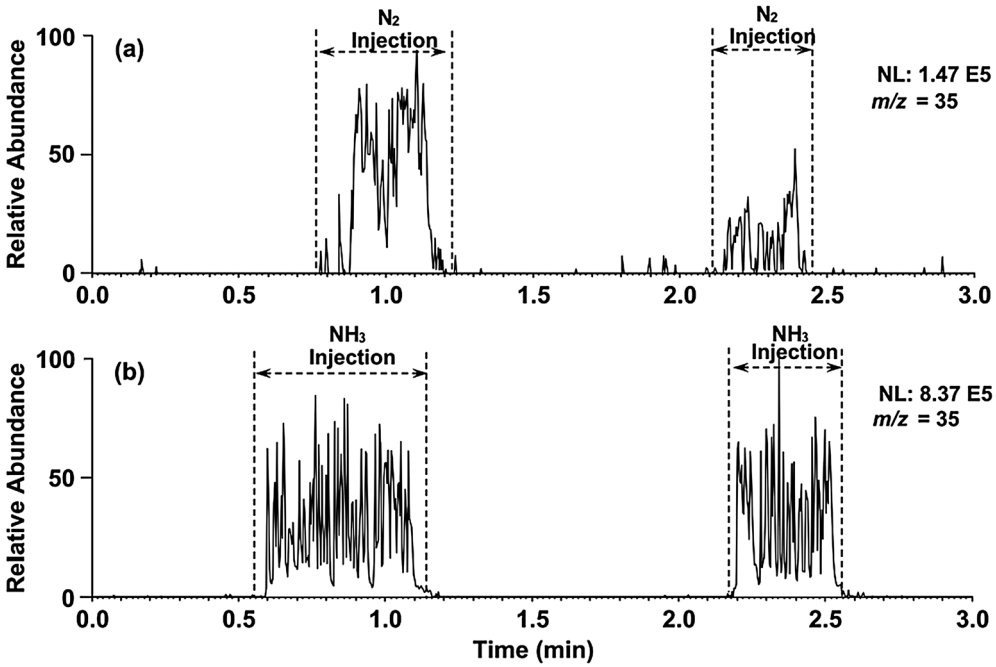

Figure 3. The change of specifical ion current (*m/z* 35, $NH_4^+NH_3$) indicates that NH_4^+ was formed when the pure (a) N_2 or (b) NH_3 was introducing into the flame of MPT.

dominant fragment ion during the low-energy collision-induced dissociation (CID) process.[40] Although the amount of reactant NH_4^+ was increased by the improved conversion from $NH_4^+(H_2O)_n$ ($n = 1, 2$) via the increasement of drying nitrogen flow rate in the background (Figure S1 in the Supporting Information), the concomitant dissociation dominates the whole process. Therefore, the net result was that the acetone was removed from the acetone–ammonium cluster. The decrease or disappearance of the corresponding signal *m/z* 76 is evident. This process is confirmed by the extracted ion chromatograms in Fig. 4(d). It shows that the intensity of the ion $[M + NH_4]^+$ (*m/z* 76) decreased sharply at the drying nitrogen flow rate of 1.5 l/min, but the ion NH_4^+ (*m/z* 18) increased at the same time. This phenomenon shows that the high flow rate-drying nitrogen from the mass spectrometer has the dissociation effect such as the low-energy CID. In Fig. 4(d), when the drying nitrogen flow rate reached 3 l/min, all the ion intensities decreased. This result is attributed to decreased ion entrance efficiency into the mass spectrometer at a higher drying gas flow rate. For the acetic acid (Fig. 4(e)–(h)), the trend for the formation of analyte ions with the drying nitrogen flow rate is same to the acetone trend. The cases for acetone and acetic acid indicate that the drying gas from the mass spectrometer plays an important role in the generation of $[M + NH_4]^+$ and $[M + H]^+$ in MPT-MS.

The detection of active components in different drugs

Over-the-counter medicines were successfully analyzed by MPT-MS. The strong signals of the intact molecule for active components were observed in the full-scan mass spectra. In Fig. 5, the most common analyte ions for the active components except ibuprofen are the protonated molecules, which are also the base peaks. In the mass spectrum of ibuprofen (Fig. 5(a)), the main analyte ions are the ammoniated molecule (*m/z* 224) and the dimer (*m/z* 430); the protonated ibuprofen is not observed. This ibuprofen result is different from some other observations for ibuprofen with ambient desorption/ionization techniques. In desorption electrospray ionization and PADI,[11] the only reported analyte ion was the protonated ibuprofen (*m/z* 207). In microplasma discharge ionization source[15] and BADCI,[33] both protonated ibuprofen and ammoniated ibuprofen existed. In Fig. 5(a), the ammonium adduct of ibuprofen dominates the spectrum, and the generation of these analyte ions is attributed to the primary ions of ammonium adducts of water.

Besides the intact analyte ions in the full-scan mass spectra, some fragment ions for the active components were also observed for MPT-MS. Figure 5(b) is the mass spectrum of chlorphenamine. The dominating ions are the protonated molecule $[M + H]^+$ (*m/z* 275) with its M + 2 isotope (*m/z* 277). The two ions have a relative abundance ratio of 3 : 1, which is due to the chlorine atom. A similar pair of isotopic peaks exists at *m/z* 230 and 232 also with a relative abundance ratio of 3 : 1. Thus, the ions of *m/z* 230 and 232 also contain one chlorine, and they are the fragment ions obtained by the loss of 45 (CH_3NHCH_3) from the protonated chlorphenamine. In Fig. 5(c), the base peak is the protonated domperidone (*m/z* 426). Its M + 2 isotope (*m/z* 428) also existed because of the chlorine in the molecule. In the lower mass range in the domperidone spectrum, a peak at *m/z* 258 is observed, but it lacks a corresponding chlorine isotope (*m/z* 260). Therefore, the ions of *m/z* 258 are believed to be obtained by the fragmentation corresponding to loss of chlorine-containing part from domperidone. The proposed dissociation pathway is shown in Fig. 5(c), and the chlorine atom is included in the lost neutral. In Fig. 5(d), the dominating ions are also the protonated diphenidol. The fragment ions at *m/z* 292 are obtained by the loss of H_2O.

A multicomponent drug capsule was analyzed by MPT-MS. The capsule contains four active components: acetaminophen, caffeine, pseudoephedrine hydrochloride, and chlorphenamine maleate. The resulting mass spectrum is shown in Fig. 6. For all the four active components, their protonated molecules could be obtained, that is, protonated acetaminophen (*m/z* 152), protonated caffeine (*m/z* 195), protonated pseudoephedrine (*m/z* 166),

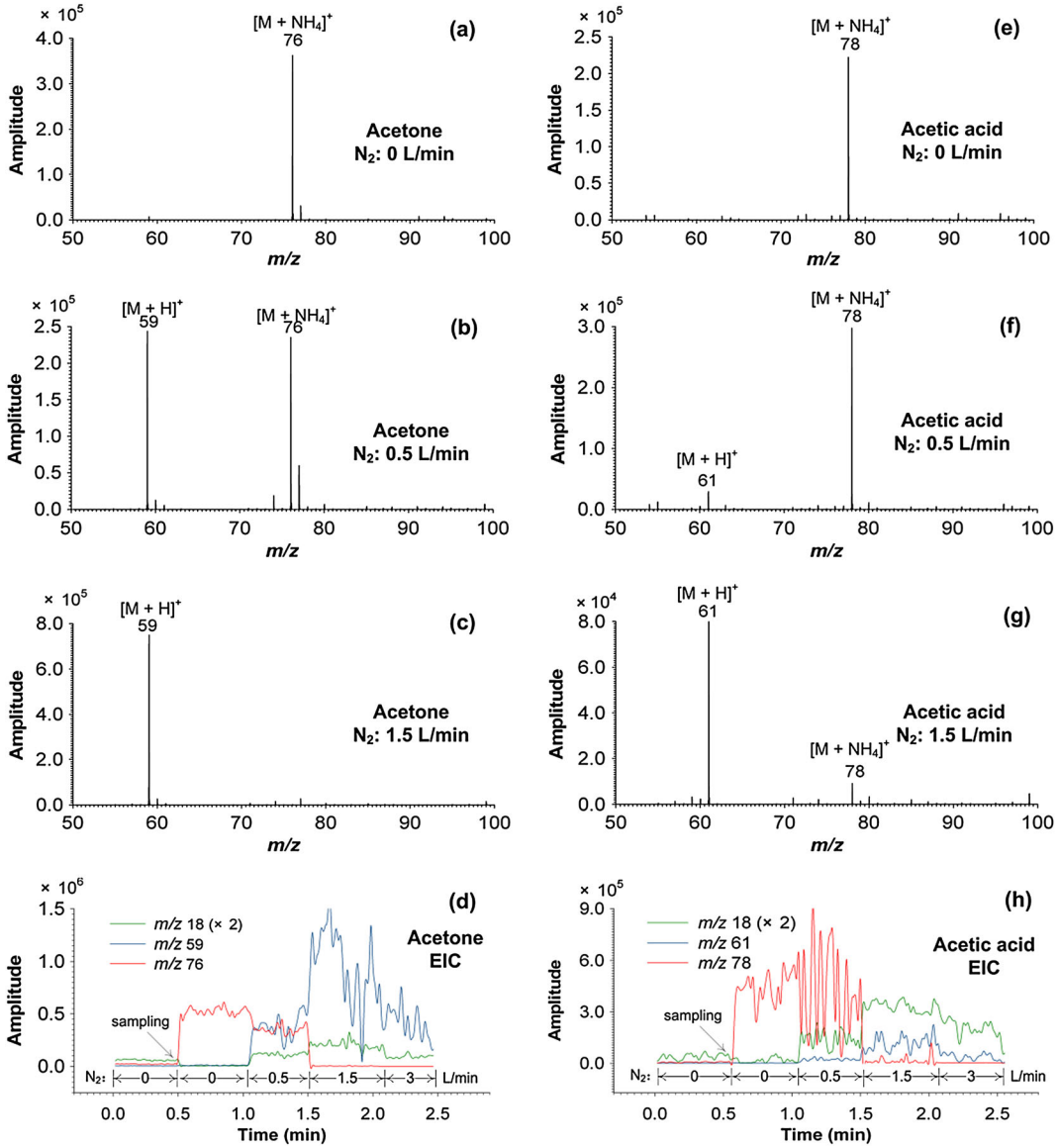

Figure 4. The mass spectra and extracted ion chromatograms (EIC) recorded by MPT-MS with four drying nitrogen flow rates for two analytes: (a)–(d) acetone and (e)–(f) acetic acid.

and protonated chlorphenamine (*m/z* 275). Interestingly, for the latter two compounds, pseudoephedrine and chlophenamine exist in the form of hydrochloride and maleate, respectively. However, by the process of the microwave plasma, the acid moieties of the pseudoephedrine hydrochloride and chlophenamine maleate were lost, and the protonated pseudoephedrine (*m/z* 166) and the protonated chlorphenamine (*m/z* 275) were observed, respectively. Fragment ions also can be observed in Fig. 6. The fragment ions of *m/z* 148 were obtained by the elimination of water from the protonated pseudoephedrine. For the chlorphenamine, the fragment ions (*m/z* 230) were obtained by the loss of CH_3NHCH_3 from the protonated chlorphenamine, and the chlorphenamine fragmentation in Figs 6 and 5(b) is the same.

Table 1 summarizes the LODs for the four active components by the MPT. Here, the calculation method referenced the one proposed by Symonds *et al.*[15] Similarly, the sample analysis region was approximated to the size of the plasma tip spot, about a 3-mm circle, on the tablet surface, and the desorption/ionization depth was estimated to be about 10 μm. The LOD (S/N = 3) was calculated on the basis of the linear correlation between analyte amount in the analysis region (3 mm circle × 10 μm thickness) and the actual signal intensity. The LOD values for four active components in four tablets are in the range of 0.5–31.7 ng/mm^2. Two reasons exist for the range. First, the inert ingredients of the medicine could affect the desorption rates of the analytes. Second, the primary ions may have different reaction rates with the analytes. Thus for various active components, the LOD values may be different, even for the same active component in different medicines. The detection limits could be improved further by refining the arrangement of the ionization source for promoting the ion transmission into the mass spectrometer.

In summary, the active components in various medicines were successfully detected by MPT-MS in ambient desorption mode. The protonated and the ammoniated molecules are the two main intact analyte ions. The fragmentation of the active components occurs easily in MPT-MS, and the fragment ions provide further evidence for the identification of the analytes. Indeed, more works are needed to develop the empirical rules for widely used applications.

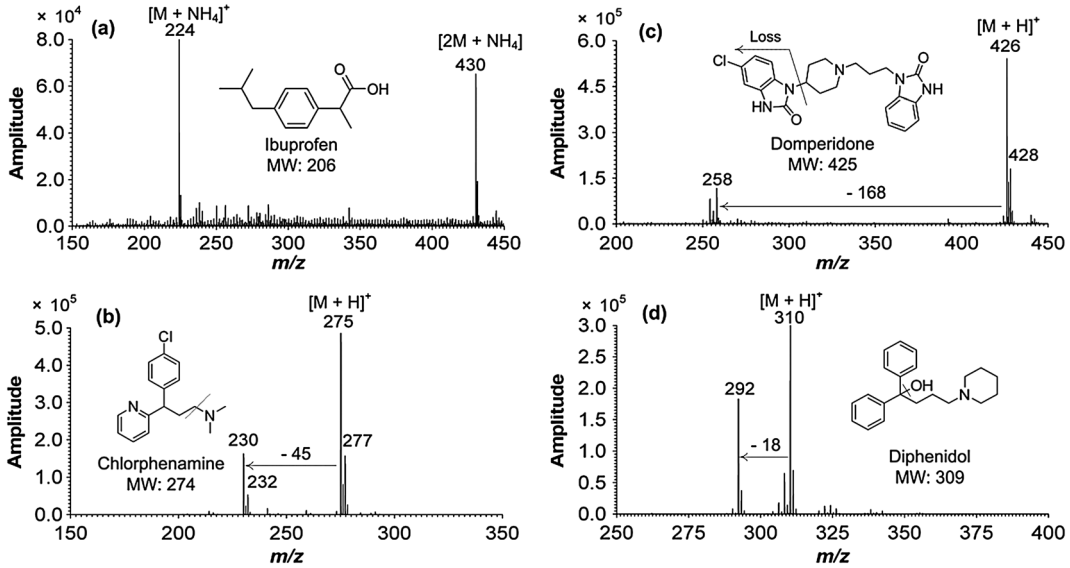

Figure 5. The full-scan mass spectra obtained by MPT-MS for medicines: (a) ibuprofen, (b) chlorphenamine, (c) domperidone, and (d) diphenidol tablets.

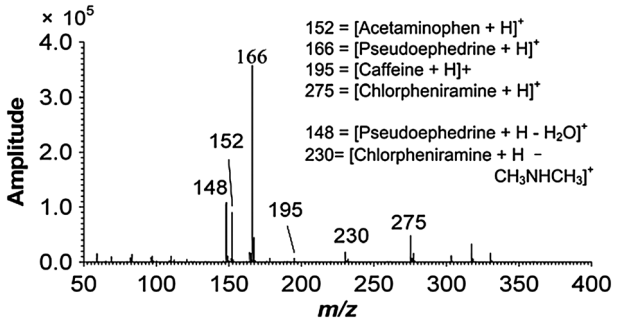

Figure 6. The full-scan mass spectra obtained by MPT-MS for multicomponent medicine: capsule of acetaminophen, caffeine, pseudoephedrine hydrochloride, and chlorphenamine maleate.

The characterization of the allicin in garlic

Allicin is one of the most abundant organo-sulfur compounds in garlic, and it has a variety of biological activities.[41–45] However, allicin is instable and reactive;[46] therefore, it is important to characterize allicin in its native conditions to avoid its loss during pretreatment. Here, direct analysis was performed to characterize allicin in fresh garlic by using MPT-MS. A garlic clove was positioned in the plasma beam after removing the peel without any pretreatment. A mass spectrum was obtained immediately and contains the predominant peak at *m/z* 163 (Fig. 7), which is identified as the protonated allicin. The appearance of the protonated allicin dimer (*m/z* 325) indicates that the allicin molecules were desorbed effectively by MPT. The successful detection of allicin in garlic indicates MPT-MS is a potential method used for direct analysis of natural products. Allicin was also detected by PADI,[11] but the fragment ions obtained by the elimination of water from the protonated allicin were much more abundant than the protonated allicin. The fragmentation of the allicin with argon-sustained MPT and the helium-induced PADI are compared. The former cannot form the fragment ions by the elimination of water, but the latter can form it. These observations with allicin suggest that the argon-sustained MPT may be softer than the helium-induced PADI under the experimental conditions.

Monitoring nicotine in exhaled breath after smoking

The gas-phase sample was easy to be analyzed by MPT-MS. Here, nicotine in exhaled breath after smoking was monitored for 20 min as a case study for gas-phase sample analysis by MPT-MS. After smoking, although exhaled breath contains complex components, the signal of nicotine is the strongest. As shown in the inset of Fig. 8, the ions of *m/z* 163 are the protonated nicotine, are evident, and are easily observed after smoking. The intensity of the protonated nicotine was used for the decay kinetics of nicotine (Fig. 8). Herein, each data point is an average of 15 s. Observed from

Table 1. The limits of detection (LODs) of different active components using the MPT[a]

Medicine	Active component	LOD (ng/mm^2) [b]
Ibuprofen tablet	Ibuprofen	31.7
Chlorphenamine maleate tablet	Chlorphenamine maleate	0.66
Difenidol hydrochloride tablet	Difenidol hydrochloride	9.0
Domperidone tablet	Domperidone	0.5

[a]The details are shown in the following text.
[b]LOD used here is expressed as the surface concentrations of active components per 1 mm^2 of tablet surface with estimated 10 μm plasma depletion layer.

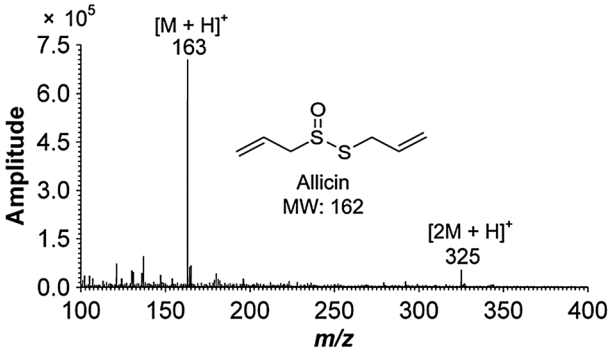

Figure 7. The mass spectrum obtained by MPT-MS for the analysis of freshly garlic.

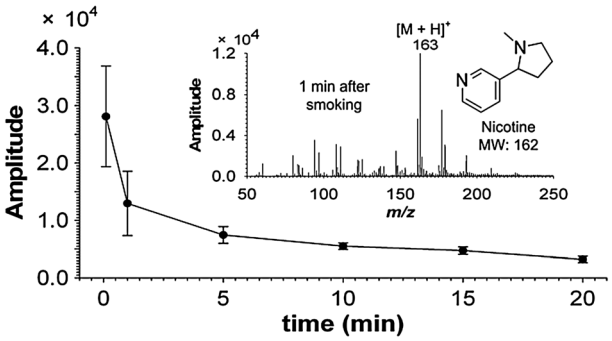

Figure 8. Decay curve of nicotine in exhaled breath after smoking by MPT-MS. The inset is the mass spectrum of the exhaled breath recorded 1 min after smoking.

this decaying curve, about 1 min after smoking, the content of nicotine decays to half. However, even up to 20 min, there is still detectable signal of nicotine. This may be due to the slow absorption of nicotine, so nicotine persists over 20 min in the body and is brought out with the exhale. This case shows that the MPT-MS is a valid tool for monitoring the targeted compound in the complex-matrix gas.

Conclusions

In conclusion, an ambient desorption/ionization source based on microwave plasma generated by MPT has been developed. Various samples have been analyzed by MPT coupled with a TOF mass spectrometer. The results show that the microwave plasma has an effective desorption/ionization capability and provides a valid method for the rapid analysis of solid samples (e.g., pharmaceuticals) and monitoring gases (e.g., exhaled breath) in real time. The results from the MPT background suggest that the H_3O^+ and NH_4^+ and the corresponding clusters are important types of primary ions in this ionization source. The flow rate of drying nitrogen from mass spectrometer is shown to be a very important factor to affect the analyte ions. Besides the two common intact analyte ions (the protonated and ammoniated adduct ions) obtained, the fragmentation of the analytes is easy to be observed in the full-scan mass spectra; to some extent, this can assist the identification of the analytes without further spectrometric experiments (such as CID). The MPT generates a stable microwave plasma at atmospheric pressure and has the advantages of the plasma-based ambient ionization techniques, such as minimal requirements for optimization of operating parameters, easy operation, no need for solvent, and no sample pretreatment. Thus, MPT-MS is a potential technique for ambient MS for the direct analysis of complex samples. Indeed, the experience rules need more further works for widely applications.

Acknowledgements

This work was supported by the National Instrumentation Program (2011YQ14015008, 2011YQ14015009), Natural Science Foundation of Jiangxi Province (2010GZH0002), and Major Science and Technology Projects of Zhejiang Province (2008C01053-5).

Supporting information

Supporting information may be found in the online version of this article.

References

[1] R. M. Alberici, R. C. Simas, G. B. Sanvido, W. Romao, P. M. Lalli, M. Benassi, I. B. S. Cunha, M. N. Eberlin. Ambient mass spectrometry: bringing MS into the "real world". *Anal. Bioanal. Chem.* **2010**, *398*, 265.
[2] R. G. Cooks, Z. Ouyang, Z. Takats, J. M. Wiseman. Ambient mass spectrometry. *Science* **2006**, *311*, 1566.
[3] Z. Takats, J. M. Wiseman, B. Gologan, R. G. Cooks. Mass spectrometry sampling under ambient conditions with desorption electrospray ionization. *Science* **2004**, *306*, 471.
[4] H. Gu, N. Xu, H. Chen. Direct analysis of biological samples using extractive electrospray ionization mass spectrometry (EESI-MS). *Anal. Bioanal. Chem.* **2012**, *403*, 2145.
[5] M. Z. Huang, S. C. Cheng, Y. T. Cho, J. Shiea. Ambient ionization mass spectrometry: a tutorial. *Anal. Chim. Acta* **2011**, *702*, 1.
[6] G. A. Harris, A. S. Galhena, F. M. Fernandez. Ambient sampling/ionization mass spectrometry: applications and current trends. *Anal. Chem.* **2011**, *83*, 4508.
[7] A. Venter, M. Nefliu, R. G. Cooks. Ambient desorption ionization mass spectrometry. *Trends Anal. Chem.* **2008**, *27*, 284.
[8] R. B. Cody, J. A. Laramée, H. D. Durst. Versatile new ion source for the analysis of materials in open air under ambient conditions. *Anal. Chem.* **2005**, *77*, 2297.
[9] Z. Takats, I. Cotte-Rodriguez, N. Talaty, H. W. Chen, R. G. Cooks. Direct, trace level detection of explosives on ambient surfaces by desorption electrospray ionization mass spectrometry. *Chem. Commun.* **2005**, 1950.
[10] N. Na, M. Zhao, S. Zhang, C. Yang, X. Zhang. Development of a dielectric barrier discharge ion source for ambient mass spectrometry. *J. Am. Soc. Mass Spectrom.* **2007**, *18*, 1859.
[11] L. V. Ratcliffe, F. J. M. Rutten, D. A. Barrett, T. Whitmore, D. Seymour, C. Greenwood, Y. Aranda-Gonzalvo, S. Robinson, M. McCoustra. Surface analysis under ambient conditions using plasma-assisted desorption/ionization mass spectrometry. *Anal. Chem.* **2007**, *79*, 6094.
[12] F. J. Andrade, J. T. Shelley, W. C. Wetzel, M. R. Webb, G. Gamez, S. J. Ray, G. M. Hieftje. Atmospheric pressure chemical ionization source. 1. Ionization of compounds in the gas phase. *Anal. Chem.* **2008**, *80*, 2646.
[13] J. D. Harper, N. A. Charipar, C. C. Mulligan, X. R. Zhang, R. G. Cooks, Z. Ouyang. Low-temperature plasma probe for ambient desorption ionization. *Anal. Chem.* **2008**, *80*, 9097.
[14] M. Taghioskoui, M. Zaghloul, A. Montaser. *Sensors, 2010 IEEE*. IEEE: Kona, HI, **2010**, 797.
[15] J. M. Symonds, A. S. Galhena, F. M. Fernandez, T. M. Orlando. Microplasma discharge ionization source for ambient mass spectrometry. *Anal. Chem.* **2010**, *82*, 621.
[16] X. Li, H. Wang, W. Sun, L. Ding. Desorption corona beam ionization coupled with a poly(dimethylsiloxane) substrate: broadening the application of ambient ionization for water samples. *Anal. Chem.* **2010**, *82*, 9188.
[17] Q. Jin, G. Yang, A. Yu, J. Liu, H. Zhang, Y. Ben. A novel plasma emission source. *J. Nat. Sci. Jinlin Univ.* **1985**, 90.

[18] Q. Jin, C. Zhu, M. W. Border, G. M. Hieftje. A microwave plasma torch assembly for atomic emission spectrometry. *Spectrochim. Acta B* **1991**, *46*, 417.
[19] K. J. Jankowski, E. Reszke. *Microwave induced plasma analytical spectrometry*, Vol. *12*. RSC, **2010**.
[20] Q. Jin, F. Wang, C. Zhu, D. M. Chambers, G. M. Hieftje. Atomic emission detector for gas chromatography and supercritical fluid chromatography. *J. Anal. Atom. Spectrom.* **1990**, *5*, 487.
[21] W. Yang, H. Zhang, A. Yu, Q. Jin. Microwave plasma torch analytical atomic spectrometry. *Microchem. J.* **2000**, *66*, 147.
[22] J. H. Barnes IV, O. A. Grøn, G. M. Hieftje. Characterization of an argon microwave plasma torch coupled to a Mattauch-Herzog geometry mass spectrometer. *J. Anal. Atom. Spectrom.* **2002**, *17*, 1132.
[23] B. W. Pack, G. M. Hieftje, Q. Jin. Use of an air/argon microwave plasma torch for the detection of tetraethyllead. *Anal. Chim. Acta* **1999**, *383*, 231.
[24] G. Feng, Y. Huan, Y. Cao, S. Wang, X. Wang, J. Jiang, A. Yu, Q. Jin, H. Yu. Development of a miniature simultaneous MPT spectrometer. *Microchem. J.* **2004**, *76*, 17.
[25] Y. Duan, Y. Su, Z. Jin, S. P. Abeln. Design and development of a highly sensitive, field portable plasma source instrument for on-line liquid stream monitoring and real-time sample analysis. *Rev. Sci. Instrum.* **2000**, *71*, 1557.
[26] J. A. C. Broekaert, N. Bings, C. Prokisch, M. Seelig. A close-up of three microwave plasma sources in view of improved element-specific detection in liquid chromatography. *Spectrochim. Acta B* **1998**, *53*, 331.
[27] M. Huang, D. Hanselman, Q. Jin, G. Hieftje. Non-thermal features of atmospheric-pressure argon and helium microwave-induced plasmas observed by laser-light Thomson scattering and Rayleigh scattering. *Spectrochim. Acta B* **1990**, *45*, 1339.
[28] M. Wu, Y. Duan, Q. Jin, G. M. Hieftje. Elemental mass spectrometry using a helium microwave plasma torch as an ion source. *Spectrochim. Acta B* **1994**, *49*, 137.
[29] G. Q. Li, Y. X. Duan, G. M. Hieftje. Space-charge effects and Ion distribution in plasma source-mass spectrometry. *J. Mass Spectrom.* **1995**, *30*, 841.
[30] Y. X. Su, Y. X. Duan, Z. Jin. Helium plasma source time-of-flight mass spectrometry: off-cone sampling for elemental analysis. *Anal. Chem.* **2000**, *72*, 2455.
[31] B. W. Pack, J. A. C. Broekaert, J. P. Guzowski, J. Poehlman, G. M. Hieftje. Determination of halogenated hydrocarbons by helium microwave plasma torch time-of-flight mass spectrometry coupled to gas chromatography. *Anal. Chem.* **1998**, *70*, 3957.
[32] J. T. Shelley, J. S. Wiley, G. C. Y. Chan, G. D. Schilling, S. J. Ray, G. M. Hieftje. Characterization of direct-current atmospheric-pressure discharges useful for ambient desorption/ionization mass spectrometry. *J. Am. Soc. Mass Spectrom.* **2009**, *20*, 837.
[33] J. Steeb, A. S. Galhena, L. Nyadong, J. Janata, F. M. Fernandez. Beta electron-assisted direct chemical ionization (BADCI) probe for ambient mass spectrometry. *Chem. Commun.* **2009**, 4699.
[34] K. Hiraoka, S. Fujimaki, S. Kambara, H. Furuya, S. Okazaki. Atmospheric-pressure Penning ionization mass spectrometry. *Rapid Commun. Mass Spectrom.* **2004**, *18*, 2323.
[35] M. Pavlik, J. D. Skalny. Generation of $[H_3O]^+.(H_2O)_n$ clusters by positive corona discharge in air. *Rapid Commun. Mass Spectrom.* **1997**, *11*, 1757.
[36] T. Fujii, K. Iwase, P. C. Selvin. Mass spectrometric analysis of a N_2/H_2 microwave discharge plasma. *Int. J. Mass. Spectrom.* **2002**, *216*, 169.
[37] J. J. Perez, G. A. Harris, J. E. Chipuk, J. S. Brodbelt, M. D. Green, C. Y. Hampton, F. M. Fernandez. Transmission-mode direct analysis in real time and desorption electrospray ionization mass spectrometry of insecticide-treated bednets for malaria control. *Analyst* **2010**, *135*, 712.
[38] E. P. L. Hunter, S. G. Lias. Evaluated gas phase basicities and proton affinities of molecules: an update. *J. Phys. Chem. Ref. Data* **1998**, *27*, 413.
[39] J. B. Westmore, M. M. Alauddin. Ammonia chemical ionization mass-spectrometry. *Mass Spectrom. Rev.* **1986**, *5*, 381.
[40] X. Li, A. G. Harrison. Structures of the adduct ions formed in the ammonia chemical ionization of ketones. *J. Am. Chem. Soc.* **1993**, *115*, 6327.
[41] S. Oommen, R. J. Anto, G. Srinivas, D. Karunagaran. Allicin (from garlic) induces caspase-mediated apoptosis in cancer cells. *Eur. J. Pharmacol.* **2004**, *485*, 97.
[42] F. Freeman, Y. Kodera. Garlic chemistry: stability of s-(2-propenyl)-2-propene-1-sulfinothioate allicin) in blood, solvents, and simulated physiological fluids. *J. Agr. Food Chem.* **1995**, *43*, 2332.
[43] L. N. Ceci, O. A. Curzio, A. B. Pomilio. Effects of irradiation and storage on the flavor of garlic bulbs cv "red". *J. Food Sci.* **1991**, *56*, 44.
[44] E. Block. The chemistry of garlic and onions. *Sci. Am.* **1985**, *252*, 114.
[45] C. J. Cavallito, J. H. Bailey. Allicin, the antibacterial principle of allium sativum I isolation, physical properties and antibacterial action. *J. Am. Chem. Soc.* **1944**, *66*, 1950.
[46] M. E. Rybak, E. M. Calvey, J. M. Harnly. Quantitative determination of allicin in garlic: supercritical fluid extraction and standard addition of alliin. *J. Agr. Food Chem.* **2004**, *52*, 682.